Surface & Coatings Technology xxx (2016) xxx–xxx

Contents lists available at ScienceDirect

Surface & Coatings Technology

journal homepage: www.elsevier.com/locate/surfcoat

Superhydrophobic Si surfaces having microscale rod structures prepared in a plasma etching system

Sung-Woon Cho [a], Jun-Hyun Kim [a], Hae-Min Lee [b], Heeyeop Chae [c], Chang-Koo Kim [a,*]

[a] Department of Chemical Engineering and Department of Energy Systems Research, Ajou University, Worldcup-ro 206, Woncheon-dong, Yeongtong-gu, Suwon 443-749, Korea
[b] Institute of NT-IT Fusion Technology, Ajou University, Worldcup-ro 206, Woncheon-dong, Yeongtong-gu, Suwon 443-749, Korea
[c] School of Chemical Engineering, Sungkyunkwan University, Seobu-ro 2066, Jangan-gu, Suwon 440-746, Korea

ARTICLE INFO

Article history:
Received 14 December 2015
Revised 25 April 2016
Accepted in revised form 4 May 2016
Available online xxxx

JEL classification:
AP 27

Keywords:
Superhydrophobic
Microscale rod
Fluorocarbon film
Plasma etching

ABSTRACT

Superhydrophobic Si surfaces (contact angle of 165°) were successfully achieved by combining the fabrication of microscale rods with the deposition of fluorocarbon films on the surface. The aspect ratio of the rod was varied in order to analyze the effect of surface roughness on the contact angle of the surface. In the absence of fluorocarbon films on the rods, the contact angle on the Si surface having microscale rod structures increased to 95° with increasing aspect ratio (of the rod) of up to 3.5. This indicated that the wetting behavior of Si surfaces having microscale rod structures was affected by a combination of the Wenzel and the Cassie-Baxter states. When a fluorocarbon film was deposited on these surfaces, the contact angle increased to 165° with increasing aspect ratio (of the rod) of up to 1.5, and remained approximately constant thereafter. Therefore, surface microstructuring (rather than nanostructuring) using a conventional plasma etching system constitutes a practical method for the realization of superhydrophobic surfaces.

1. Introduction

The superhydrophobicity of solid surfaces with contact angles above 150° is essential for practical applications such as self-cleaning and anti-fogging surfaces, DNA arrays, and microfluidics [1–4]. The hydrophobicity depends on the chemical composition and roughness of the solid surface. Many techniques, including the use of surface coating and surface nanostructuring, have been proposed for the control of this property [5–11].

Surface coating with hydrophobic materials constitutes a simple and easy means of modifying the chemical composition of the surface. However, this method has limitations to realize superhydrophobic surfaces (contact angle >150°). Many researchers have proposed the use of novel materials (such as fluorocarbon films that have low surface energies) for the fabrication of hydrophobic surfaces [5–7]. However, these novel materials give rise to water contact angles of only 110–120°.

Superhydrophobicity can be achieved through surface nanostructuring, which is used to fabricate one-dimensional (1-D) nanoscale structures, such as nanorods and nanowires, on the surfaces of interest [8–10]. Fan et al. obtained superhydrophobic surfaces with Si nanorods that were fabricated via oblique angle deposition and subsequently fluorinated by using a HF solution [8]. Egatz-Gomez et al. produced superhydrophobic surfaces with perfluoroctyltriethoxysilane-coated Si nanowires fabricated via a chemical etching method [9]. In addition, by using a plasma, Tserepi et al. examined the variation in the contact angle on polydimethyl siloxane (PDMS) surfaces consisting of nanorods. They reported that stable superhydorphobic surfaces could be obtained when the height of the rod was > 500 nm [10]. However, the fabrication of uniformly arrayed nanoscale structures on a solid surface is extremely difficult. Moreover, superhydrophobic surfaces obtained via surface nanostructuring exhibit limited resistance to mechanical abrasion [11].

Microscale structures are more easily prepared than nanoscale structures and hence microscale surface texturing (i.e., surface microstructuring) constitutes a promising alternative to surface nanostructuring for the fabrication of superhydrophobic surfaces. In fact, patterning of microscale structures using plasma etching has been well developed in the area of microelectronic devices for decades. This implies that the use of microscale structures for the realization of superhydrophobic surfaces has significant potential for commercialization. There are, however, only a few studies on the superhydrophobicity of surfaces consisting of microscale structures.

In this work, Si surfaces having microscale rod structures were fabricated via plasma etching, and their superhydrophobicity was investigated. The aspect ratio of the rods was varied in order to analyze the effect of the surface roughness on the contact angle of the surface. Moreover, fluorocarbon films were deposited on the Si surfaces having microscale rod structures in order to investigate the effect of surface energy on the hydrophobicity of the surface.

* Corresponding author.
E-mail address: changkoo@ajou.ac.kr (C.-K. Kim).

http://dx.doi.org/10.1016/j.surfcoat.2016.05.009
0257-8972/© 2016 Elsevier B.V. All rights reserved.

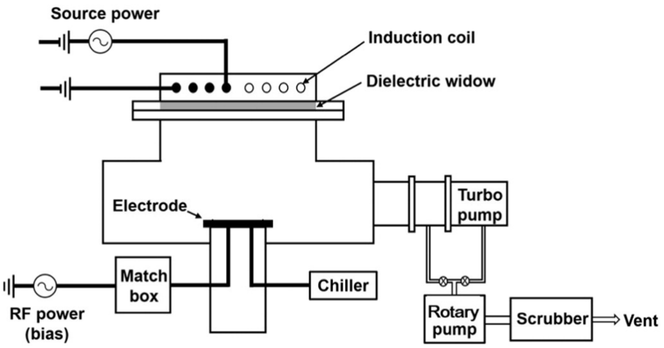

Fig. 1. A schematic of an inductively coupled plasma system used for the fabrication of microscale rod structures and the deposition of fluorocarbon films on the Si surfaces.

2. Experiment

2.1. Fabrication of microscale rod structures of Si

An inductively coupled plasma (ICP) system (Fig. 1) was used to produce a high density plasma for the fabrication of microscale rod structures on Si surfaces. The reaction chamber was made of stainless steel. Separate 13.56 MHz radio frequency (RF) power generators were used independently to ignite a plasma and bias a substrate, respectively. The source power was applied to an induction coil, whereas the bias power was applied via a stainless-steel electrode. A quartz dielectric window was located below the induction coil, and the distance between the dielectric window and the electrode was 100 mm.

Microscale rod structures were fabricated on a p-type Si (100) wafer that was cut into a 10 × 10 mm^2 rectangle. Fig. 2 shows the scanning electron microscopy (SEM) images of the samples. The Si substrate had a convex SiO_2-mask hole pattern. The diameters of the holes were 2, 4, 8, and 10 μm, respectively. The pitch of each pattern was two times larger than the hole diameter and hence the patterns were spaced 2, 4, 8, and 10 μm apart, respectively. The height of the hole pattern was 2 μm in all substrates.

Etching was performed via a so-called deep Si etching, which is a cyclic process consisting of alternating etching and deposition steps. SF_6 and C_4F_8 plasmas were used in the etching and deposition steps, respectively. The source power and bias voltage were 800 W and −50 V, respectively, in the etching step while 800 W and 0 V, respectively, in the deposition step. In the etching step, the flow rate of SF_6 was 30 sccm, and the chamber pressure was 10 mTorr. In the deposition step, the flow rate of C_4F_8 was 30 sccm, and the chamber pressure was 30 mTorr. The durations of etching and deposition steps were 40 and 10 s, respectively. Deep Si etching was carried out for 12, 24, 36, and 48 cycles, respectively, to obtain various heights of the rods.

After the deep Si etching, the samples were ashed at 500 °C for 1 h in order to remove the residual fluorocarbon films formed on the rods. The SiO_2 masks were removed by wet chemical etching in a HF solution for 2.5 min, and the samples were subsequently rinsed with deionized water in an ultrasonicator (JAC-1505, KODO) for 5 min.

Fig. 3 shows the SEM images of the Si surface with microscale rod structures that were fabricated in this study. The cross-sectional SEM images are shown in the insets. The heights of the rods were 4, 7.2, 11.5, and 15.4 μm after 12, 24, 36, and 48 cycles of deep Si etching, respectively, and were the same irrespective of the rod diameters. This resulted in uniform etch rats of around 300 nm/cycle. Moreover, Si surfaces having highly anisotropic and uniformly arrayed microscale rods, with aspect ratios ranging from 0.4 to 7.7, were obtained via conventional deep Si etching.

2.2. Deposition of fluorocarbon films

Fluorocarbon films were deposited on the microscale rod structures of Si in order to investigate the effect of the surface energy on the hydrophobicity of the surface. Deposition of the fluorocarbon films was carried out using a C_4F_8 plasma in the ICP system shown in Fig. 1. The source power and bias voltage were 800 W and 0 V, respectively. The flow rate of C_4F_8 was 30 sccm. The chamber pressure was 30 mTorr, and deposition time was 7 s.

2.3. Measurement of the contact angle

Water contact angles were measured using a contact angle meter (P-CAM, GIT Soft), which was equipped with a video camera. A 0.5-μL water droplet, whose volume was precisely controlled by a microliter syringe (7000.5 KH SYR, Hamilton), was placed on the Si surface. The contact angles were measured three times for each sample and were averaged to obtain the final data.

3. Results and discussion

Fig. 4 shows the images of water droplets on the Si surfaces that have microscale rods of various diameters and heights. The rods are spaced at distances equal to their diameters. For a fixed height of the rod, the contact angle decreases with increasing diameter of the rod. For example, at a rod height of 4 μm, the contact angle decreases from 90 to 69° with increasing rod diameter from 2 to 10 μm. The magnitude of this decrease becomes progressively lower, however, with increasing height of the rods. This indicates that the surface roughness plays an important role in the wetting behavior of the Si surface that consists of microscale rod structures. This role was elucidated by using the aspect ratio (i.e., the height of a rod divided by its diameter) as a measure of the surface roughness. Note that the space between the rods has the same

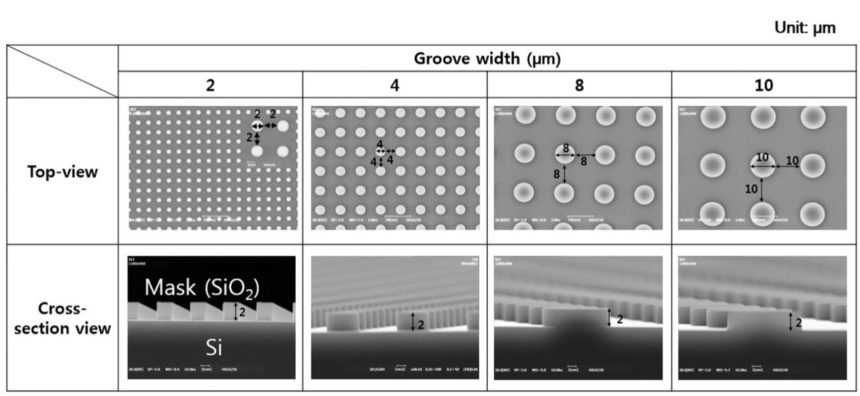

Fig. 2. SEM images of the hole patterns on the samples. SiO_2 was used as a mask.

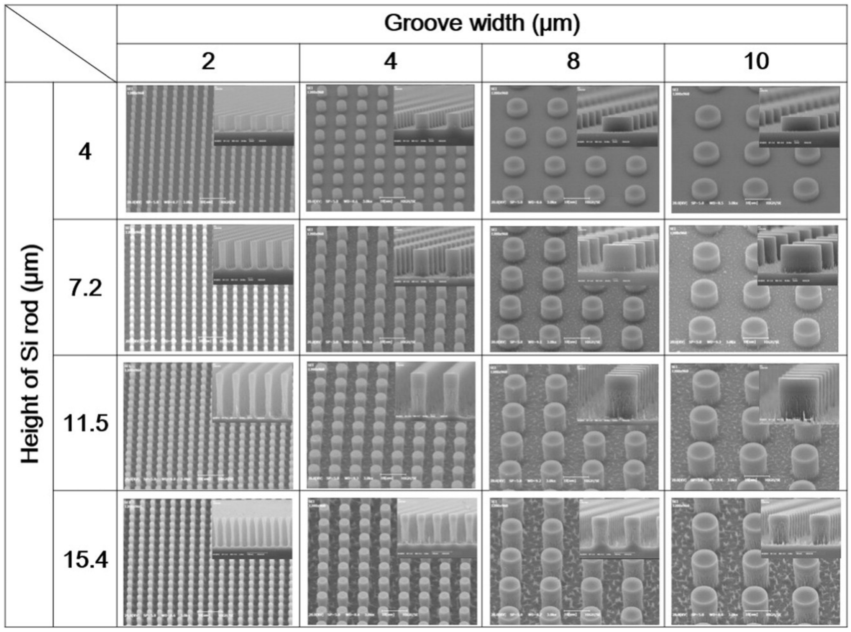

Fig. 3. SEM images of the Si surfaces having microscale rod structures obtained after deep Si etching. The insets show the corresponding cross-sectional SEM images. SEM was taken after the residual fluorocarbon films and SiO_2 masks were removed.

aspect ratio as the rods since the diameter of, and spacing between, the rods are identical.

Fig. 5 shows the contact angles on the aforementioned Si surfaces. Note that the contact angle on the bare Si surface (no microscale rods) was 46°. When the Si surfaces are microstructured with rods having aspect ratios of 0.4, the contact angle greatly increases to 69°. The contact angle increases from 69 to 95° as the aspect ratio of the rod increases from 0.4 to 3.5, then it remains approximately constant (i.e., at 95°) with aspect ratios higher than 3.5.

The variation in the contact angle on a rough surface is described by the classical Wenzel and Cassie-Baxter models [12,13]. In the Wenzel model, a liquid droplet wets the entire solid surface and fills the gap in the texture (referred to as homogeneous wetting). According to the Wenzel model, an originally hydrophilic surface (contact angle <90°) becomes more hydrophilic and a hydrophobic surface (contact angle >90°) becomes more hydrophobic with increasing roughness [14]. On the other hand, the Cassie-Baxter model describes that a water droplet sits on the top of the texture, and leaves air pockets inside the cavity (referred to as heterogeneous wetting).

As seen in Fig. 5, the contact angle increases with increasing aspect ratio of 0.4–3.5. If the wetting behavior in this regime fulfills the stipulations of the Wenzel model, then the contact angle should decrease with increasing aspect ratio, owing to the hydrophilicity of the Si surface. However, the contact angle increases (Fig. 5), indicating that the wetting behavior on the Si surfaces having microscale rod structures does not conform to the Wenzel model. The wetting state on a rough surface can transit from the Wenzel to the Cassie-Baxter state, with increasing surface roughness (or aspect ratio of the textures) [15–17]. Consider the case where the wetting state lies in the transition regime between the Wenzel and Cassie states. In this case, the contact angle increases owing to the combined effect of these states. Suh and Jon evaluated the wettability of polyethylene glycol (PEG) surfaces and found

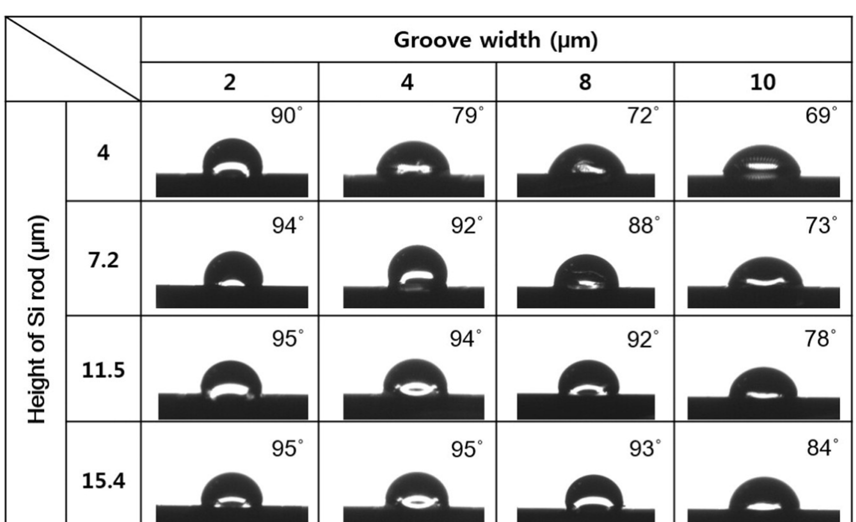

Fig. 4. Images of 0.5-μL water droplets on Si surfaces having microscale rod structures. The corresponding contact angles are given in each image.

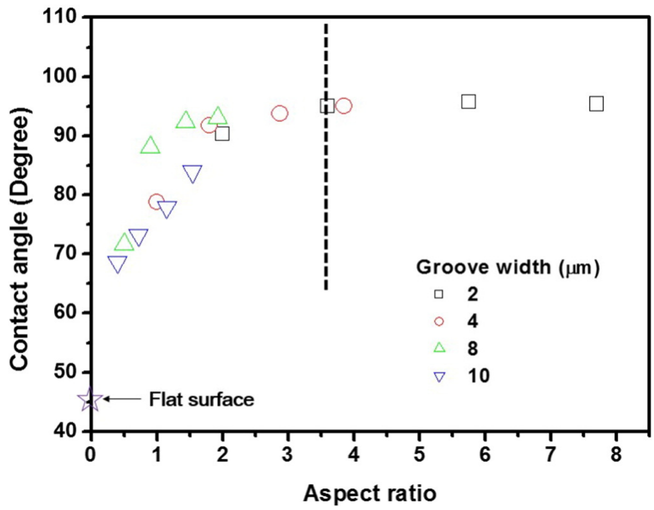

Fig. 5. Contact angles on the Si surfaces having microscale rods of various aspect ratios.

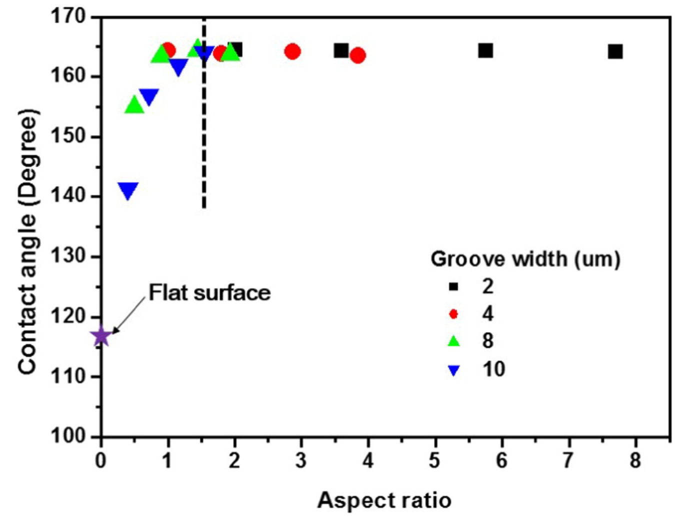

Fig. 7. Contact angles as a function of the aspect ratio of the rod, for Si surfaces having microscale rods and subsequently deposited fluorocarbon films.

that the contact angle on hydrophilic surfaces increased with increasing aspect ratio of the nanostructures [15]. Ishino et al. reported that the air-pocket state could be observed on a hydrophilic surface decorated with rods, and energy barriers prevented complete wetting of the liquid-solid surfaces [16,17]. These studies indicate that variations in the contact angle on a hydrophilic surface cannot be explained solely by the Wenzel or Cassie-Baxter model. Therefore, at aspect ratios lower than 3.5, the wettability of the Si surfaces having microscale rod structures might be affected by a combination of the Wenzel and Cassie-Baxter states.

The contact angle on the Si surface having microscale rods increased to a value of ~95° at an aspect ratio of 3.5 and remained constant thereafter. A continuous increase in the contact angle with increasing aspect ratio was expected. The saturation of the contact angle at aspect ratios higher than 3.5 results possibly from the surface energy of Si (2130 mJ/m^2) [18]. In other words, the sufficiently high surface energy prevents further penetration of the water droplet into the cavity.

Using conventional plasma etching, an increase in the contact angle on the Si surface was easily achieved by texturing the surface with microscale rod structures. The maximum contact angle obtained (i.e., ~95°) is, however, inadequate for practical applications. In order to enhance the hydrophobicity of the surface, fluorocarbon films, which have low surface energy, were subsequently deposited on the rods. Deposition of fluorocarbon films was performed in the ICP system (shown in Fig. 1) using a C_4F_8 plasma. These films should have no effect on the aspect ratio of the rods. The thickness of the fluorocarbon films was measured at various deposition times, and it was 65-nm for 10 s-deposition. Considering that the Si rods were on a few micrometer scale, deposition of 65 nm-thick fluorocarbon film would have negligible effect on the aspect ratio of the rods. Therefore, a deposition time of 10 s was used.

Fig. 6a shows the X-ray photoelectron spectroscopy (XPS) survey scan of the fluorocarbon films deposited on the rods. These measurements were performed on a Si surface that consists of 2 μm (diameter) × 15.4 μm (height) rods. The corresponding C1 s and F1 s peaks occur at binding energies of 291.5 and 689.1 eV, respectively. However, the Si 2p peak (typical binding energy of ~100 eV) is absent [19]. This indicates that the Si surface is perfectly covered by the fluorocarbon film. The high-resolution C1 s spectrum (Fig. 6b) exhibits peaks at 287.8, 289.8, 292.4, and 294.5 eV, which are attributed to the C-CF$_x$, CF, CF$_2$, and CF$_3$, respectively [20–22]. From the C1 s XPS spectrum, a surface coverage (i.e., F/(F + C)) of the fluorocarbon film is calculated to be 0.44 [22].

Yosida et al. investigated the hydrophobicity of fluorocarbon polymers and examined the relationship between the surface coverage and the surface energy [7]. They demonstrated that the concentration of F had a direct effect on the hydrophobicity of a flat fluorocarbon polymer surface. Based on the results of their study, a surface energy of ~10 mJ/m^2 is estimated for the fluorocarbon film deposited in this work.

Fig. 7 shows the contact angle as a function of aspect ratio of the rods, for Si surfaces having microscale rods on which fluorocarbon films were deposited. Note that the flat surface in the figure represents the bare Si surface (no microscale rods) on which the fluorocarbon films were deposited. The film leads to an increase in the contact angle, as evidenced by the significantly higher contact angle (116°) of the flat surface than

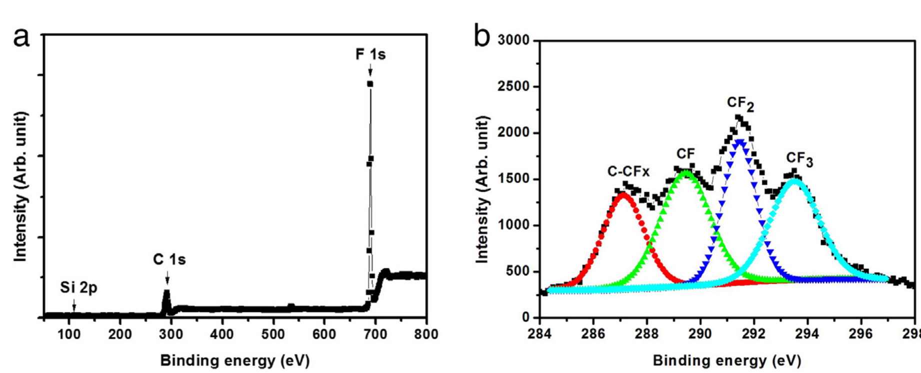

Fig. 6. (a) XPS survey scan and (b) high-resolution C1 s XPS spectra of the fluorocarbon films deposited on the microscale Si rods. The deconvolution (thin lines) of the spectra in (b) was conducted by using a linear background and Gaussian functions.

Please cite this article as: S.-W. Cho, et al., Surf. Coat. Technol. (2016), http://dx.doi.org/10.1016/j.surfcoat.2016.05.009

that (46°) of the bare surface without the film. The contact angle on the microtextured surface with the film is even higher. For example, contact angles of 141° and 165° are obtained when the film is deposited on surfaces with rods having aspect ratios of 0.4 and 1.5, respectively. A contact angle of 165° indicates that the surface is superhydrophobic (contact angle >150°). Moreover, as the figure shows, the contact angle is approximately constant for aspect ratios higher than 1.5. The realization of a superhydrophobic Si surface via the deposition of a fluorocarbon film implies that air is trapped between the water droplet (liquid) and the Si surface (solid). This superhydrophobicity results from the sufficiently small surface energy, thereby leading to the formation of a composite solid-liquid-air interface. Therefore, by combining the fabrication of microscale rod structures and the deposition of fluorocarbon films on Si surfaces, a superhydrophobic Si surface was achieved in a plasma etching system.

4. Conclusions

The hydrophobicity of Si surfaces having highly anisotropic and uniformly arrayed microscale rod structures, fabricated via conventional deep Si etching, was investigated. The contact angle (69°) measured on the Si surface microstructured with even low-aspect-ratio rods (i.e., rods with aspect ratio of, for example, 0.4) was higher than that (46°) of the bare surface. The contact angle on the Si surfaces having microscale rod structures increased from 69 to 95° with increasing aspect ratio of 0.4–3.5. This increase indicated that the wetting behavior of these surfaces might be governed by a combination of the Wenzel and Cassie-Baxter states. Furthermore, owing to the high surface energy of Si, a constant contact angle of ~95° was obtained at aspect ratios higher than 3.5.

The hydrophobicity of the Si surface having microscale rod structures was enhanced by depositing fluorocarbon films on the rods. The contact angle increased to a value of 165° with increasing aspect ratio (of up to 1.5) of the rods and remained approximately constant thereafter.

By combining the fabrication of microscale rod structures and the deposition of fluorocarbon films on the Si surface, a superhydrophobic Si surface with a contact angle of 165° was successfully achieved via plasma etching. This indicates that surface microstructuring, whose preparation and control are easier than those of nanostructuring, constitutes a feasible method for realizing a superhydrophobic Si surface.

Acknowledgements

This work was supported by the National Research Foundation of Korea (NRF) grant funded by the Korea government (MEST) (Grant Nos. 2015R1A2A2A01002305 and NRF-2009-0094046), and by the Industrial Strategic Technology Development Program (Grant No. 10041681, Development of fundamental technology for 10 nm process semiconductor and 10 G size large area process with high plasma density and VHF condition) funded by the Korea government (MOTIE).

References

[1] M. Callies, D. Quéré, On water repellency, Soft Matter 1 (2005) 55–61.
[2] Y. Lai, Y. Tang, J. Gong, D. Gong, L. Chi, C. Lin, Z. Chen, Transparent superhydrophobic/superhydrophilic TiO_2-based coatings for self-cleaning and anti-fogging, J. Mater. Chem. 22 (2012) 7420–7426.
[3] S.D. Gillmor, A.J. Thiel, T.C. Strother, L.M. Smith, M.G. Lagally, Hydrophilic/hydrophobic patterned surfaces as templates for DNA arrays, Langmuir 16 (2000) 7223–7228.
[4] V. Srinivasan, V.K. Pamula, R.B. Fair, An integrated digital microfluidic lab-on-a-chip for clinical diagnostics on human physiological fluids, Lab Chip 4 (2004) 310–315.
[5] T. Nishino, M. Meguro, K. Nakamae, M. Matsushita, Y. Ueda, The lowest surface free energy based on $-CF_3$ alignment, Langmuir 15 (1999) 4321–4323.
[6] J.-H. Wang, J.-J. Chen, R.B. Timmons, Plasma synthesis of a novel CF_3-dominated fluorocarbon film, Chem. Mater. 8 (1996) 2212–2214.
[7] N. Yoshida, Y. Abe, H. Shigeta, A. Nakajima, H. Ohsaki, K. Hashimoto, T. Watanabe, Sliding behavior of water droplets on flat polymer surface, J. Am. Chem. Soc. 128 (2006) 743–747.
[8] J.-G. Fan, X.-J. Tang, Y.-P. Zhao, Water contact angles of vertically aligned Si nanorod arrays, Nanotechnology 15 (2004) 501–504.
[9] A. Egatz-Gomez, R. Majithia, C. Levert, K.E. Meissner, Super-wetting, wafer-sized silicon nanowire surfaces with hierarchical roughness and low defects, RSC Adv. 2 (2012) 11472–11480.
[10] A.D. Tserepi, M.-E. Vlachopoulou, E. Gogolides, Nanotexturing of poly (dimethylsiloxane) in plasmas for creating robust super-hydrophobic surface, Nanotechnology 17 (2006) 3977–3983.
[11] Y. Xiu, Y. Liu, D.W. Hess, C.P. Wong, Mechanically robust superhydrophobicity on hierarchically structured Si surfaces, Nanotechnology 21 (2010) 155705.
[12] R.N. Wenzel, Resistance of solid surfaces to wetting by water, Ind. Eng. Chem. 28 (1936) 988–994.
[13] A.B.D. Cassie, S. Baxter, Wettability of porous surfaces, Trans. Faraday Soc. 40 (1944) 546–551.
[14] M. Nosonovsky, B. Bhushan, Roughness optimization for biomimetic superhydrophobic surfaces, Microsyst. Technol. 11 (2005) 535–549.
[15] K.Y. Suh, S. Jon, Control over wettability of polyethylene glycol surfaces using capillary lithography, Langmuir 21 (2005) 6836–6841.
[16] C. Ishino, K. Okumura, Wetting transitions on textured hydrophilic surfaces, Eur. Phys. J. E 25 (2008) 415–424.
[17] C. Ishino, K. Okumura, D. Quéré, Wetting transitions on rough surfaces, Europhys. Lett. 68 (2004) 419–425.
[18] R.J. Jaccodine, Surface energy of germanium and silicon, J. Electrochem. Soc. 110 (1963) 524–527.
[19] B.R. Weinberger, G.G. Peterson, T.C. Eschrich, H.A. Krasinski, Surface chemistry of HF passivated silicon: X-ray photoelectron and ion scattering spectroscopy results, J. Appl. Phys. 60 (1986) 3232–3234.
[20] T.E.F.M. Standaert, C. Hedlund, E.A. Joseph, G.S. Oehrlein, T.J. Dalton, Role of fluorocarbon film formation in the etching of silicon, silicon dioxide, silicon nitride, and amorphous hydrogenated silicon carbide, J. Vac. Sci. Technol. A 22 (2004) 53–60.
[21] N. Takada, T. Iida, K. Shibagaki, K. Sasaki, Chemical bonds of fluorocarbon films which can be a source of CF_x radicals, J. Vac. Sci. Technol. A 22 (2004) 413–418.
[22] K. Takahashi, K. Tachibana, Molecular composition of films and solid particles polymerized in fluorocarbon plasmas, J. Appl. Phys. 89 (2001) 893–899.